Biogeosciences
Discussions

Open Access

Ba, B, and U element partitioning in magnesian calcite skeletons of Octocorallia corals

T. Yoshimura[1], A. Suzuki[2], and N. Iwasaki[3]

[1]Japan Agency for Marine-Earth Science and Technology 2–15, Natsushima-cho, Yokosuka-city, Kanagawa 237-0061, Japan
[2]Geological Survey of Japan, National Institute of Advanced Industrial Science and Technology, Tsukuba Central 7, 1-1-1 Higashi, Tsukuba, Ibaraki 305-8567, Japan
[3]Faculty of Geo-Environmental Science, Rissho University, Magechi 1700, Kumagaya, Saitama 360-0194, Japan

Correspondence to: T. Yoshimura (yoshimurat@jamstec.go.jp)

Abstract

Barium, boron and uranium element partitioning and oxygen and carbon isotope fractionation of high-Mg calcite skeletons of Octocorallia corals were investigated. The dissolved Ba concentration in seawater and the coral Ba / Ca ratio showed a clear positive correlation. The empirically derived barium partition coefficient is comparable to previous data for not only calcitic corals but also intermediate- to deep-water-dwelling scleractinian corals whose skeletons are composed of aragonite. Octocorallia corals are geologically important producers of biominerals, and they provide long-term records (up to hundreds of years) of environmental conditions in the deep ocean. Our data suggest that Ba / Ca ratios in Octocorallia corals may be a useful proxy for nutrients in intermediate and deep waters. The Ba / Ca ratio, a possible proxy for pH or carbonate ion concentration in seawater, showed the largest correlation with $\delta^{13}C$ among the examined parameters. This result implies that the pH of the extracytoplasmic calcifying fluid (ECF) simultaneously influences $\delta^{18}O$, $\delta^{13}C$, and Ba / Ca by influencing the relative contributions of dissolved carbon sources in the ECF. Positive correlations of Ba / Ca with δ^{18} and $\delta^{13}C$ suggest that δ^{18} and $\delta^{13}C$ are enriched in light isotopes when conditions are less alkaline, suggesting a potential role of biological alkalinity pumping becomes more favorable with decreasing calcifying fluid pH. Substantial inter- and intra-specimen variations in Ba / Ca suggest that physicochemical factors do not exert a dominant systematic control on U incorporation.

1 Introduction

The chemical compositions of the hard parts of calcifying organisms, such as coral skeletons and foraminifer, brachiopod, and mollusk shells, are crucial as tracers of past environmental conditions. Calcium carbonate ($CaCO_3$) is one of the most abundant biominerals, and the chemical composition, ultrastructure, and organic components of carbonate minerals ultimately determine their physicochemical properties. Corals

are a geologically important producer of biominerals that provide long-term records of environmental conditions over a wide range of water depths, from the surface to deep water. Non-symbiotic corals, which are distributed at water depths ranging from several dozen to thousands of meters (Iwasaki, 2010), can provide millennial-scale records of

5 environmental conditions in intermediate and deep waters (e.g., Smith et al., 1997; Adkins et al., 1998; Sherwood et al., 2005; Eltgroth et al., 2006; Montagna et al., 2006; van de Flierdt et al., 2006). Octocorallia (Anthozoa) coral skeletons are composed of high-Mg calcite, and the longevity of these corals means that they can provide long-term records of environmental conditions.

10 The use of minor and trace metal compositions of biogenic $CaCO_3$ as proxies for paleoenvironmental conditions has also been of great value. Despite their potential utility for decadal- to centennial-scale records in intermediate and deep waters, however, only a few studies, have investigated depth-sensitive trace-element partitioning of calcitic corals (LaVigne et al., 2011; Sinclair et al., 2011; McCulloch et al., 2012).

15 Intermediate- and deep-water chemistry are affected by decadal-scale climate changes via changes in ocean circulation and ventilation and in biochemical and geochemical cycling. The dissolved barium concentration in the ocean shows significant variations that depend on water depth and locality, and it behaves similarly to nutrients such as dissolved silica (e.g., Bacon and Edmond, 1972). Therefore, barium concentrations are

20 higher in deep waters and in areas of nutrient upwelling. Moreover, Ba/Ca ratios in the skeletons of calcitic corals can be reliably used as a proxy for nutrients in the intermediate water masses in which such corals live (Sinclair et al., 2011; LaVigne et al., 2011; Hasegawa et al., 2012).

In addition, pH-sensitive tracers such as boron isotopes and B/Ca (Foster et al.,

25 2008; Allen and Hönisch, 2012), and U/Ca (Reeder et al., 2000; Russell et al., 2004; Inoue et al., 2011) have been used to study past ocean pH. These tracers are linked to the ocean's inorganic carbon cycle, which plays a central role in climate change. Boron-based pH proxies rely on the fact that the relative abundances and B isotopic compositions of the two aqueous species of boron in seawater, $B(OH)_3$ and $B(OH)_4^{2-}$,

Full Screen / Esc

Printer-friendly Version

Interactive Discussion

are pH dependent (e.g., Kakihana et al., 1977). Data on boron partitioning in inorganic calcite show that changes in the relative proportions of these dissolved species are clearly recorded in the B/Ca ratio and that $B(OH)_4^{2-}$ is the dominant species incorporated into the calcite structure (Sanyal et al., 2000). Recently, robust pH tracers for use in paleoceanography have been explored by a biological species-specific approach (e.g., Allen and Hönisch, 2012, and references therein), but only one study has examined boron isotopes in calcite skeletons of intermediate- and deep-water-dwelling corals (McCulloch et al., 2012), and that study did not systematically evaluate the B/Ca ratio of calcitic corals.

In this study, we investigated B, Ba, and U element partitioning in the calcite skeletons of Octocorallia corals collected from sites at a range of water depths. Our aim was to investigate whether past environmental changes can be inferred from Ba/Ca, B/Ca, and U/Ca values recorded in deep-sea coral skeletons.

2   Materials and methods

We selected 13 specimens of deep-sea coral (*Paracorallium japonicum*, *Corallium elatius*, *C. konojoi*, *Corallium* sp., and *Keratoisis* sp.) from several sampling localities at water depths of 30–1500 m in the western, northwestern, and northern Pacific (Table 1). Mean annual water temperatures at the sampling localities range from 2.5 to 19.5 °C (water temperatures are from Levitus94; http://ingrid.ldeo.columbia.edu/ SOURCES/.LEVITUS94/) (Levitus and Boyer, 1994). The coral skeletons were ground to powder in an agate mortar before analysis. The Mg/Ca ratios and the Mg isotope ratios of these specimens have already been reported by Yoshimura et al. (2011). In addition, a semi-fossilized coral skeleton (*Corallium elatius*) collected at 200–300 m depth at 25° N, 126° E was cut perpendicular to the growth axis and a dental drill was used to sample the skeleton along the maximum growth line from the central axis to the outer margin at 1 mm intervals in order to examine intra-specimen changes in trace metal profiles (Fig. 1).

Oxygen and carbon isotope ratios were measured with an isotope ratio mass spectrometer (Micromass ISOPRIME) at the National Institute for Advanced Industrial Science and Technology. Isotopic data are reported as per mil (‰) deviations relative to Vienna Peedee Belemnite (VPDB). The NBS-19 carbonate standard was used for calibration of the VPDB scale. Analytical precision was ±0.1‰ for both δ^{18}O and δ^{13}C.

The ratios of minor and trace elements to Ca were measured with a quadrupole inductively coupled plasma mass spectrometer (iCAP Qc; Thermo Scientific, Bremen, Germany) at the Japan Agency for Marine-Earth Science and Technology and calibrated using the JCp-1 (prepared from a modern reef-building coral) and JCt-1 (Holocene fossil giant clam shell) carbonate reference materials from the Geological Survey of Japan (Okai et al., 2004) and mono-element standard reagents from Kanto Chemical. To reduce Ca matrix effects and control for instrumental drift, internal standards (Be, Sc, Y, and In) were added to the solution. Additionally, standard solutions were measured after every fifth sample for data correction. All element concentrations are given as molar ratios relative to Ca.

For proxy evaluations (see Table 2), we used δ^{18}O, δ^{13}C, and $[CO_3^{2-}]$ data from the inorganic carbon chemistry database, Global Ocean Data Analysis Project (GLODAP, http://cdiac.ornl.gov/oceans/glodap/; Key et al., 2004). The δ^{18}O values used were 0‰ for most samples, and +0.2‰ for DPC-V1 and DPC-V4. We selected δ^{13}C, alkalinity, and dissolved inorganic carbon (DIC) data that had been collected at points in the Pacific Ocean close to the deep-sea coral sampling localities, and we calculated other inorganic carbon data with the CO2SYS program (Lewis and Wallace, 1998). Dissolved barium concentrations ($[Ba]_{sw}$) determined at habitat depths near the coral sampling locations were used for calibration of the barium partitioning coefficient (Oba and Kato, 2012). To calculate fractionation and partitioning coefficients, we used values based on δ^{13}C–depth and $[Ba]_{sw}$–depth relationships determined near the coral sampling sites (Fig. 2).

Full Screen / Esc

Printer-friendly Version

Interactive Discussion

3 Results

3.1 Trace element concentrations

The profiles of inorganic carbon dioxide and of oceanic tracers with nutrient-like behaviors in ambient seawater changed markedly with depth. The B/Ca, Ba/Ca, and U/Ca ratios of the suite of Octocorallia corals were plotted in relation to the habitat depths of the corals (Fig. 3). B/Ca and U/Ca values ranged from 0.104 to 0.252 mmol mol^{-1}, and from 0.007 to 0.093 µmol mol^{-1}, respectively (Fig. 3), and substantial interspecimen differences were observed in both ratios at each habitat depth. Nevertheless, both elements tended to be negatively related to water depth. Such inverse relationships with depth might reflect a positive relationship between these ratios and ambient water temperature or inorganic carbon chemistry, and B/Ca and U/Ca showed moderate correlations with some habitat environmental parameters (Table 2).

Unlike B/Ca and U/Ca, Ba/Ca exhibited a clear increasing trend with depth, and interspecimen differences were small (Fig. 3). To evaluate Ba/Ca partitioning in the skeletons, we used dissolved Ba concentrations in seawater measured at Northwest Pacific sites nearest to the coral sampling locations (Oba and Kato, 2012). The dissolved Ba concentration increased from the surface to 1000 m depth by a factor of ~ 3 (Fig. 2, black squares), and Ba/Ca in the coral skeletons showed a strong positive correlation with the ambient dissolved Ba ([Ba]$_{SW}$) ($r = 0.95$; $p < 0.0001$; Fig. 4). The following equation was obtained by linear regression:

$$\text{Ba/Ca}_{coral} = (0.127 \pm 0.012) \cdot [\text{Ba}]_{sw} - (0.093 \pm 0.688) \tag{1}$$

The central axis of the skeleton of the semi-fossilized *C. elatius* (DPC-15) was characterized by higher B/Ca and Ba/Ca, and lower U/Ca, compared with their values in more marginal samples, and clear growth bands were apparent along the growth axis (Fig. 5). In this specimen, B/Ca ranged from 0.102 to 0.166 mmol mol^{-1} and Ba/Ca ranged from 4.361 to 5.261 µmol mol^{-1}, and both B and Ba concentrations were markedly higher at the central axis (Fig. 5, Table 3). In the outer part of the skeleton,

however, B and Ba showed relatively small variability, indicating that on the whole, their concentrations remained the same throughout the life of the coral. In contrast, U/Ca showed a clear increasing trend from 0.034 to 0.326 µmol mol^{-1} with growth of the coral, although it decreased to ~ 0.23 µmol mol^{-1} near the margin of the specimen (Fig. 5). Average Mg/Ca ratios were stable (average, around 126 mmol mol^{-1}) along the sampling transect, but they showed an overall seasonal variation of 5.9 % relative to the average.

3.2 Trace element concentrations

The oxygen and carbon isotope data of the specimens are previously published in Yoshimura et al. (2015). In the coral skeletons, δ^{18}O varied from −2.38 to −0.74 ‰, and δ^{13}C varied from −6.12 to 0.00 ‰ (Table 1). We observed a large interspecimen variation in the relationship between these isotope ratios and water depths (Fig. 3). The Mg content of calcite is known to substantially increase the isotope fractionation factor α at a given temperature (Tarutani et al., 1969; Jimenez-Lopez et al., 2004; Mavromatis et al., 2012). Therefore, to estimate the influence of Mg on isotope fractionation in the corals, we first calculated the difference values (δ^{18}O$_{coral}$ − δ^{18}O$_{calc}$, δ^{13}C$_{coral}$ − δ^{13}C$_{calc}$), where δ^{18}O$_{coral}$ and δ^{13}C$_{coral}$ are the observed isotopic compositions of the corals, and δ^{18}O$_{calc}$ and δ^{13}C$_{calc}$ are those estimated by examining the effect of both temperature and Mg content on calcite–fluid isotope fractionation equilibria in synthetic magnesian calcite (Jimenez-Lopez et al., 2006; Mavromatis et al., 2012).

In the coral samples, the Mg/Ca ratio ranged from 73.75 to 137.40 mmol mol^{-1} and showed a clear positive correlation with water temperature (Yoshimura et al., 2011). Previous studies have examined the effect of Mg on oxygen isotope fractionation equilibria by theoretical calculations (Schauble et al., 2006; Chacko and Deines, 2008), but these theoretical models tend to underestimate the effect of Mg at lower temperatures and to overestimate its effect at higher temperatures, relative to data obtained empirically by experimental precipitation of magnesian calcite (Mavromatis et al., 2012).

If we estimate the effect of the Mg content by using the empirically determined oxygen and carbon isotope fractionation factors reported by Mavromatis et al. (2012) and Jimenez-Lopez et al. (2006), the resulting difference values for δ^{18}O and δ^{13}C range from −4.66 to −1.53 and from −7.34 to −1.75, respectively (Table 1, Yoshimura et al., 2015). These results indicate that both the oxygen and carbon isotope ratios of the calcitic corals in this study were depleted in heavier isotopes compared with the ratios of inorganic magnesian calcite.

4 Discussion

4.1 Ba/Ca as a proxy for past nutrient status

4.1.1 Calibration regressions

Ba/Ca ratios in coral skeletons of various taxa have been used as a proxy for nutrient load in the ocean (McCulloch et al., 2003; Montaggioni et al., 2006). Oceanic barium and silica are similarly distributed in the water column and both show a nutrient-like behavior, having higher concentrations in areas of high productivity. In this study, the change in skeletal Ba/Ca with depth parallels that in the dissolved barium concentration in Pacific seawater (Fig. 2; Bernat et al., 1972; Chan et al., 1976; Oba and Kato, 2013), and our results are in excellent agreement with earlier results for gorgonian corals (LaVigne et al., 2011; Sinclair et al., 2011). Regression Eq. (1) obtained in this study is very similar to that reported for gorgonian corals (LaVigne et al., 2011), the skeletons of which are also composed of high-Mg calcite. Both previously published data and our data show strong positive linear correlations between the Ba/Ca ratio in corals of multiple taxa and the dissolved Ba concentration in seawater (Fig. 4), as follows:

$$\text{Ba/Ca}_{\text{coral}} = (0.092 \pm 0.013) \cdot [\text{Ba}]_{\text{sw}} + (2.246 \pm 1.334) \tag{2}$$

where $r = 0.906$, $n = 46$, and $p < 0.001$. Moreover, this multi-taxa calibration equation obtained using the data by this study and by LaVigne et al. (2011) agrees well with the observed Ba partitioning in scleractinian cold-water coral skeletons (*Desmophyllum*; Anagnostou et al., 2011):

$$Ba/Ca_{coral} = (0.104 \pm 0.024) \cdot [Ba]_{sw} + (2.415 \pm 1.536) \tag{3}$$

Generally speaking, the distribution coefficients of minor elements in calcium carbonates are strongly controlled by the lattice structures of calcite and aragonite, the predominant polymorphs of biogenic $CaCO_3$, where calcite has a hexagonal and aragonite an orthorhombic structure. Despite the differences in the carbonate mineralogy of calcitic and aragonitic corals, however, Ba partitioning behavior is surprisingly similar between them. This fact has already been pointed out by LaVigne et al. (2011), who concluded that the skeletal Ba incorporation mechanism must be relatively simple, without any strong biological or taxonomic influences or dependence on temperature, salinity, or carbonate ion concentrations. Because neither mineral-specific nor species-specific partitioning is observed, the use of Ba/Ca ratios in both calcitic and aragonitic intermediate- and deep-water corals as an indicator of dissolved Ba is justifiable if the skeletal portion to be analyzed is carefully selected, as discussed in the following section.

4.1.2 Ba incorporation mechanisms

Because the ultimate aim is to more accurately calculate changes in paleonutrient dynamics in intermediate and deep waters, the intraskeletal distributions of Ba, B, U, and Mg were measured along the growth transect of the semi-fossilized *C. elatius* specimen (Fig. 5). Elevated Ba/Ca ratios were observed at the central axis of the skeleton, and similar Ba enrichment has been reported previously in particular skeletal microstructures and along the central axis in bamboo corals (Sinclair et al., 2011; LaVigne et al., 2011), despite differences in sample types and habitat environments. Repeated observations of Ba enrichment along the skeletal axis suggests a biological artifact. For

example, Ba-bearing organic matter or other mineral phases may occur along the central axis (e.g., Nothdurft et al., 2005; Allison et al., 2007) as a result of different modes of skeletal growth. In this regard, LaVigne et al. (2011) suggested that the association between the skeletal central axis and higher Ba/Ca ratios might be attributable to the presence of organic-rich calcite deposited during the juvenile stage of skeletal growth (Noé and Dullo, 2006). The localized occurrence of elevated Ba spanning a few millimeters along the central axis (Fig. 5) might affect the accuracy and precision of quantitative $[Ba^{2+}]$ reconstruction and lead to the overestimation of past ocean Ba concentrations.

The use of Ba/Ca as a proxy is based on the assumption that mineralogical factors, rather than the biological factors mentioned above, dominantly control Ba incorporation, but possible mineralogical factors have not been well examined at the molecular scale (Finch et al., 2010, and references therein). The ionic radius of Ba^{2+} (1.47 Å) is larger than that of Ca^{2+} (1.18 Å). As a result, Ba is thought to preferentially coprecipitate with aragonite over calcite, because the aragonite structure allows incorporation of larger ions into the crystal lattice. Inorganic coprecipitation of Ba with $CaCO_3$ is well studied, and the concentration of Ba in aragonite is approximately two orders of magnitude higher than its concentration in calcite (e.g., Kitano et al., 1971; Tesoriero and Pankow, 1996; Dietzel et al., 2004). These results are inconsistent with the finding of no apparent differences in Ba partitioning between calcitic and aragonitic corals.

The Mg content of calcite can be low or high, and the amount of Mg incorporated into the crystal lattice of calcite influences its physicochemical properties. For example, the Mg content affects thermodynamic stability and step morphology of calcite as well as the rate of crystal growth during $CaCO_3$ precipitation (e.g., Mucci and Morse, 1983; Davis et al., 2000; Morse et al., 2007). The incorporation of Ba into low-Mg calcite foraminiferal shells is known to be an order of magnitude smaller than that into high-Mg-calcite coral skeletons (Hönisch et al., 2011), but data on the crystallographic control of Ba incorporation in high-Mg calcite are still scarce. Tamenori et al. (2014) suggested that crystal lattice distortion induced by the presence of minor elements

influence minor- and trace-element incorporation; for example, the substitution of tetra-
hedral sulfate for planar carbonate ions causes distortion of the calcite unit cell along
the c. axis and allows the substitution of other elements for Ca ions (Kontrec et al.,
2004). The spatial distributions of minor elements such as magnesium and sulfate
5 in the coral skeleton are closely related (Vielzeuf et al., 2013; Tamenori et al., 2014;
Nguyen et al., 2014), and the distribution of Ba may be governed partly by the influ-
ence of other important minor elements. Analyses of the microscale distributions of
trace and minor elements and of in situ chemical speciation are needed to investigate
the robustness of key environmental parameters affecting the composition of the coral
10 skeleton.

Many marine organisms do not directly record local environmental parameters in
their biominerals, because they produce their biominerals under strict biological con-
trols (so-called vital effects). Nevertheless, the excellent empirical agreement between
dissolved Ba in seawater and the Ba/Ca ratio in multiple taxa of calcitic corals sug-
15 gests that skeletal the Ba/Ca of deep-sea corals is a valuable proxy for the nutrient
status in deep waters of the paleo-ocean.

4.2 Biological controls on boron and uranium partitioning

4.2.1 Do B/Ca and U/Ca reflect the pH of the ECF?

B/Ca partitioning during inorganic calcite growth in the laboratory shows a significant
20 sensitivity to changes in pH and the carbonate ion concentration in the ambient fluid
(Sanyal et al., 2000). Furthermore, observed increases in B/Ca of biogenic and in-
organic carbonates with increasing pH is related to changes in the $[B(OH)_4^-]/[HCO_3^-]$
ratio (Yu and Elderfield, 2007). Because the basis of the B/Ca pH proxy of marine car-
bonates is the dependence of pH on the relative proportions of dissolved boron species
25 in seawater, the large variation in B/Ca observed in coral skeletons should relate to the
inorganic carbon chemistry during calcification (Fig. 3).

In reef-building corals, variations of δ^{11}B, which is regarded as the best pH indicator, are controlled principally by biological factors via modification of the pH near calcification sites (Rollin-Bard et al., 2003). As in intermediate-depth and deep-water corals, in aragonitic corals the pH–δ^{11}B curve lies above the pH-dependent inorganic seawater borate equilibrium curve. However, the calcitic coral *Corallium* sp. specimen measured by McCulloch et al. has a significantly low δ^{11}B, corresponding to a theoretical pH of ∼ 0.3, compared with aragonitic corals, and also a low B concentration (McCulloch et al., 2012). This marked difference between aragonitic and calcitic corals implies that the ability of this calcitic coral species to regulate the pH of the calcifying fluid is much less (McCulloch et al., 2012). A large biological control of δ^{11}B variation has also been reported for foraminiferal calcite (Allen and Hönisch, 2012). Possible alternative controlling factors, other than ambient pH, are ambient temperature, calcification rate, and in vivo microenvironments (Ni et al., 2007; Yu et al., 2007; Tripati et al., 2011; Allen and Hönisch, 2012). Because the depth profile of dissolved B species is linked to large changes in the carbonate system and is affected to some extent by water temperature, it is difficult to separate pH effects from direct temperature effects in the natural specimens used in the present study. However, the high B/Ca variability at a certain habitat depths (Fig. 3) suggests that B/Ca profiles in calcitic corals may be primarily a result of strong biological controls rather than temperature effects. At present, because B/Ca ratios seem to be consequences of ECF conditions rather than of seawater chemistry, any environmental effects were likely overridden by biological processes. Further validation, for example, by demonstrating in situ δ^{11}B and δ^{18}O systematics as has been done in reef-building corals (Rollin-Bard et al., 2003), is needed. Thus, better understanding of the incorporation of boron into calcitic coral skeletons is a challenging problem awaiting future research.

Like B/Ca, U/Ca is a candidate pH proxy that also showed significant interspecimen variation in this study (Fig. 3). Although seawater temperature and pH may contribute to skeletal U/Ca ratios (Reeder et al., 2000; Russell et al., 2004; Inoue et al., 2011), the intra- and intercolony variation of U/Ca cannot be attributed to variations in

Full Screen / Esc

Printer-friendly Version

Interactive Discussion

environmental parameters. In the semi-fossilized specimen DPC-15, U/Ca increased markedly, by a factor of ~ 10, from the central axis to the margin (Fig. 5, Table 3). Large-amplitude variations, which were not reproduced along different measurement transects in the U/Ca profile of a bamboo coral, possibly reflected early diagenesis of the coral specimen (Sinclair et al., 2011). Moreover, uranium is readily leachable from calcite because of its disordered coordination environment in the calcite crystal (Reeder et al., 2000). A possible mechanism accounting for the observed variation of U/Ca may include controls of calcifying fluid chemistry during uranium incorporation into ECF or high-Mg calcite as observed in the B incorporation.

4.2.2 δ^{18}O and δ^{13}C disequilibrium and mechanisms of boron element partitioning

A significant variability of oxygen and carbon isotope fractionation, and the fractionation factors calculated for the corals exceeded the expected values calculated from environmental signals (Yoshimura et al., 2015), after taking into account their dependence on temperature and Mg contents (Jimenez-Lopez et al., 2006; Mavromatis et al., 2012). Skeletal δ^{18}O and δ^{13}C values are biased particularly by the inorganic carbon dynamics, which are affected by the coral calcification physiology (Cohen and McConnaughey, 2003; Adkins et al., 2003; Rollin-Bard et al., 2003). The relationship between the stable isotope ratios of carbon and oxygen is strongly linear in aragonitic corals (e.g., McConnaughey, 1989; Adkins et al., 2003). Simultaneous depletion of δ^{18}O and δ^{13}C in calcitic coral skeletons was observed relative to the calculated isotopic compositions for synthetic high-Mg calcite (Table 1, Yoshimura et al., 2015), and intra-individual δ^{18}O and δ^{13}C values also show a linear relationship in corals with high-Mg calcite skeleton (Hill et al., 2011; Kimball et al., 2014).

Because O and C isotope fractionation shows strong linear correlation in both aragonitic and calcitic corals that grow at intermediate and deep depths, the degree of biological control on isotope fractionation in aragonite and calcite must be similar. Adkins et al. (2003) proposed the existence of an interplay between two carbon pools, (1)

425

dissolved carbon entering the calcification sites by diffusion through the calicoblastic cell wall (CO_2-ccw) and (2) seawater DIC leak, during the mineralization process in the semi-isolated calcification space. Because coral internal processes probably control the isotopic composition of the coral skeleton (Yoshimura et al., 2015), the key to understanding skeletal $\delta^{18}O$ and $\delta^{13}C$ values is information about the coral calcification physiology.

In corals living at intermediate and deep depths, differences in the availability of nutrients at habitat water depths may affect coral calcification rates. The relationship between water depth and previously reported skeletal growth rates of calcitic Octocorallia coral taxa (Griffin and Druffel, 1989; Druffel et al., 1990; Garrabou and Harmelin, 2002; Marschal et al., 2004; Andrews et al., 2005; Bramanti et al., 2005; Roark et al., 2006; Bruckner and Roberts, 2009; Gallmetzer et al., 2010; Nguyen et al., 2013; Vielzeuf et al., 2013) (Fig. 6) indicates a growth rate decrease per meter of depth. Despite the large habitat depth range represented by these corals, however, the variations in the isotope ratios were greater at some depths than they were between the surface and the deepest depths. The supposed relationship between water depth and higher pH or $CaCO_3$ saturation state of the extracytoplasmic calcifying fluid (ECF), calcification would be enhanced and growth rates would be higher, but the variation in local habitat characteristics and individual corals can account for the large variation in growth rates and $\delta^{18}O$ and $\delta^{13}C$ at certain depths.

As previously discussed, corals regularly experience fluctuations in multiple environmental and physiological parameters that affect variations in calcifying fluid pH. Among the parameters studied, B/Ca showed the highest correlation with $\delta^{13}C$ (Table 2), and $\delta^{18}O$ also showed a moderate positive correlation with boron. If B/Ca is assumed to be a function of the pH of the ECF, then light isotopes would be enriched in the calcifying fluid under less alkaline conditions, because B/Ca is positively correlated with $\delta^{18}O$ and $\delta^{13}C$ values (Table 2). Assuming the existence of an interplay between two carbon pools, these results suggests that declines in calcifying fluid pH were accompanied by the higher [CO_2-ccw] contributions relative to isotopically heavy seawater DIC, sug-

gesting a potential role of biological alkalinity pumping becomes more favorable with decreasing calcifying fluid pH (Yoshimura et al., 2015). These findings imply that ECF conditions influenced both B element partitioning and O and C isotopic compositions simultaneously via variations in the dissolved carbon dynamics in the coral calcifying fluid. Corals exert stronger physiological control on their calcifying fluid pH by the ability to up-regulate pH at the site of calcification (McCulloch et al., 2012; Anagnostou et al., 2012; Venn et al., 2013). Our data on inter-colony variations suggest that differences in a biologically induced pH gradient in the calcifying region can explain a large variability of the boron partitioning behavior in high-Mg-calcite coral skeletons.

References

Adkins, J. F., Cheng, H., Boyle, E. A., Druffel, E. R., and Edwards, R. L.: Deep-sea coral evidence for rapid change in ventilation of the deep North Atlantic 15,400 years ago, Science, 280, 725–728, 1998.

Adkins, J. F., Boyle, E. A., Curry, W. B., and Lutringer, A.: Stable isotopes in deep-sea corals and a new mechanism for "vital effects", Geochim. Cosmochim. Ac., 67, 1129–1143, 2003.

Allen, K. A. and Hönisch, B.: The planktic foraminiferal B/Ca proxy for seawater carbonate chemistry: a critical evaluation, Earth Planet. Sc. Lett., 345, 203–211, 2012.

Allison, N., Finch, A. A., Webster, J. M., and Clague, D. A.: Palaeoenvironmental records from fossil corals: the effects of submarine diagenesis on temperature and climate estimates, Geochim. Cosmochim. Ac., 71, 4693–4703, 2007.

Anagnostou, E., Sherrell, R. M., Gagnon, A., LaVigne, M., Field, M. P., and McDonough, W. F.: Seawater nutrient and carbonate ion concentrations recorded as P/Ca, Ba/Ca, and U/Ca

Full Screen / Esc

Printer-friendly Version

Interactive Discussion

in the deep-sea coral *Desmophyllum dianthus*, Geochim. Cosmochim. Ac., 75, 2529–2543, 2011.

Anagnostou, E., Huang, K. F., You, C. F., Sikes, E. L., and Sherrell, R. M.: Evaluation of boron isotope ratio as a pH proxy in the deep sea coral *Desmophyllum dianthus*: evidence of physiological pH adjustment, Earth Planet. Sc. Lett., 349, 251–260, 2012.

Andrews, A. H., Cailliet, G. M., Kerr, L. A., Coale, K. H., Lundstrom, C., and DeVogelaere, A. P.: Investigations of age and growth for three deep-sea corals from the Davidson Seamount off central California, in: Cold-water Corals and Ecosystems, Springer-Verlag, Berlin, Heidelberg, 1021–1038, 2005.

Bacon, M. P. and Edmond, J. M.: Barium at GEOSECS III in the South Pacific, Earth Planet. Sc. Lett., 16, 66–74, 1972.

Bender, M., Snead, T., Chan, L. H., Bacon, M. P., and Edmond, J. M.: Barium intercalibration at Geosecs I and III, Earth Planet. Sc. Lett., 16, 81–83, 1972.

Bernat, M., Church, T., and Allegre, C. J.: Barium and strontium concentrations in Pacific and Mediterranean sea water profiles by direct isotope dilution mass spectrometry, Earth Planet. Sc. Lett., 16, 75–80, 1972.

Bramanti, L., Magagnini, G., De Maio, L., and Santangelo, G.: Recruitment, early survival and growth of the Mediterranean red coral *Corallium rubrum* (L 1758), a 4-year study, J. Exp. Mar. Biol. Ecol., 314, 69–78, 2005.

Bruckner, A. W. and Roberts, G. G. (Eds.): Proceedings of the First International Workshop on Corallium Science, Management, and Trade, U.S. Department of Commerce, Silver Spring, Hong Kong, 2009.

Chacko, T. and Deines, P.: Theoretical calculation of oxygen isotope fractionation factors in carbonate systems, Geochim. Cosmochim. Ac., 72, 3642–3660, 2008.

Chan, L. H., Edmond, J. M., Stallard, R. F., Broecker, W. S., Chung, Y. C., Weiss, R. F., and Ku, T. L.: Radium and barium at GEOSECS stations in the Atlantic and Pacific, Earth Planet. Sc. Lett., 32, 258–267, 1976.

Cohen, A. L. and McConnaughey, T. A.: Geochemical perspectives on coral mineralization, Rev. Mineral. Geochem., 54, 151–187, 2003.

Davis, K. J., Dove, P. M., and De Yereo, J. J.: The role of Mg^{2+} as an impurity in calcite growth, Science, 290, 1134–1137, 2000.

Dietzel, M., Gussone, N., and Eisenhauer, A.: Co-precipitation of Sr^{2+} and Ba^{2+} with aragonite by membrane diffusion of CO_2 between 10 and 50 °C, Chem. Geol., 203, 139–151, 2004.

Druffel, E. R., King, L. L., Belastock, R. A., and Buesseler, K. O.: Growth rate of a deep-sea coral using ^{210}Pb and other isotopes, Geochim. Cosmochim. Ac., 54, 1493–1499, 1990.

Eltgroth, S. F., Adkins, J. F., Robinson, L. F., Southon, J., and Kashgarian, M.: A deep-sea coral record of North Atlantic radiocarbon through the Younger Dryas: evidence for intermediate water/deepwater reorganization, Paleoceanography, 21, PA4207, doi:10.1029/2005PA001192, 2006.

Finch, A. A., Allison, N., Steaggles, H., Wood, C. V., and Mosselmans, J. F. W.: Ba XAFS in Ba-rich standard minerals and the potential for determining Ba structural state in calcium carbonate, Chem. Geol., 270, 179–185, 2010.

Foster, G. L.: Seawater pH, pCO$_2$ and [CO$_3^{2-}$] variations in the Caribbean Sea over the last 130 kyr: a boron isotope and B/Ca study of planktic foraminifera, Earth Planet. Sc. Lett., 271, 254–266, 2008.

Gallmetzer, I., Haselmair, A., and Velimirov, B.: Slow growth and early sexual maturity: bane and boon for the red coral *Corallium rubrum*, Estuar. Coast. Shelf S., 90, 1–10, 2010.

Garrabou, J. and Harmelin, J. G.: A 20-year study on life-history traits of a harvested long-lived temperate coral in the NW Mediterranean: insights into conservation and management needs, J. Anim. Ecol., 71, 966–978, 2002.

Griffin, S. and Druffel, E. R.: Sources of carbon to deep sea corals, Radiocarbon, 31, 533–543, 1989.

Hasegawa, H., Rahman, M. A, Luan, N. T., Maki, T., and Iwasaki, N.: Trace elements in *Corallium* spp. as indicators for origin and habitat, J. Exp. Mar. Biol. Ecol., 414–415, 1–5, 2012.

Heikoop, J. M., Hickmott, D. D., Risk, M. J., Shearer, C. K., and Atudorei, V.: Potential climate signals from the deep-sea gorgonian coral *Primnoa resedaeformis*, Hydrobiologia, 471, 117–124, 2002.

Hill, T. M., Spero, H. J., Guilderson, T., LaVigne, M., Clague, D., Macalello, S., and Jang, N.: Temperature and vital effect controls on bamboo coral (*Isididae*) isotope geochemistry: a test of the "lines method", Geochem. Geophy. Geosy., 12, Q04008, doi:10.1029/2010GC003443, 2011.

Hönisch, B., Allen, K. A., Russell, A. D., Eggins, S. M., Bijma, J., Spero, H. J., Lea, D. W., and Yu, J.: Planktic foraminifers as recorders of seawater Ba/Ca, Mar. Micropaleontol., 79, 52–57, 2011.

Title Page

Abstract | Introduction

Conclusions | References

Tables | Figures

◀◀ | ▶▶

◀ | ▶

Back | Close

Full Screen / Esc

Printer-friendly Version

Interactive Discussion

Inoue, M., Suwa, R., Suzuki, A., Sakai, K., and Kawahata, H.: Effects of seawater pH on growth and skeletal U/Ca ratios of *Acropora digitifera* coral polyps, Geophys. Res. Lett., 38, L12809, doi:10.1029/2011GL047786, 2011.

Iwasaki, N. (Ed.): A Biohistory of Precious Corals: Scientific, Cultural and Historical Perspectives, Tokai University Press, Japan, 2010.

Jimenez-Lopez, C., Romanek, C. S., Huertas, F. J., Ohmoto, H., and Caballero, E.: Oxygen isotope fractionation in synthetic magnesian calcite, Geochim. Cosmochim. Ac., 68, 3367–3377, 2004.

Jimenez-Lopez, C., Romanek, C. S., and Caballero, E.: Carbon isotope fractionation in synthetic magnesian calcite, Geochim. Cosmochim. Ac., 70, 1163–1171, 2006.

Kakihana, H., Kotaka, M., Satoh, S., Nomura, M., and Okamoto, M.: Fundamental studies on the ion-exchange separation of boron isotopes, Chem. Soc. Jpn., B50, 158–163, 1977.

Key, R. M., Kozyr, A., Sabine, C. L., Lee, K., Wanninkhof, R., Bullister, J. L., Feely, R. A., Millero, F. J., Mordy, C., and Peng, T.-H.: A global ocean carbon climatology: results from Global Data Analysis Project (GLODAP), Global Biogeochem. Cy., 18, GB4031, doi:10.1029/2004GB002247, 2004.

Kimball, J. B., Dunbar, R. B., and Guilderson, T. P.: Oxygen and carbon isotope fractionation in calcitic deep-sea corals: implications for paleotemperature reconstruction, Chem. Geol., 381, 223–233, 2014.

Kitano, Y., Kanamori, N., and Oomori, T.: Measurements of distribution coefficients of strontium and barium carbonates between carbonate precipitate and solution – abnormally high values of distribution coefficients measured at early stages of carbonate formation, Geochem. J., 4, 183–206, 1971.

Kontrec, J., Kralj, D., Brečević, L., Falini, G., Fermani, S., Noethig-Laslo, V., and Mirosavljević, K.: Incorporation of inorganic anions in calcite, Eur. J. Inorg. Chem., 23, 4579–4585, 2004.

LaVigne, M., Hill, T. M., Spero, H. J., and Guilderson, T. P.: Bamboo coral Ba/Ca: calibration of a new deep ocean refractory nutrient proxy, Earth Planet. Sc. Lett., 312, 506–515, 2011.

Levitus, S. and Boyer, T. P.: World Ocean Atlas 1994, vol. 4: Temperature, 1994.

Lewis, E. and Wallace, D. W. R.: CO2SYS – Program Developed for the CO_2 System Calculations, Carbon Dioxide Inf. Anal. Center; Report, ORNL/CDIAC-105, 1998.

Title Page

Abstract | Introduction

Conclusions | References

Tables | Figures

◄ | ►

◄ | ►

Back | Close

Full Screen / Esc

Printer-friendly Version

Interactive Discussion

Marschal, C., Garrabou, J., Harmelin, J. G., and Pichon, M.: A new method for measuring growth and age in the precious red coral *Corallium rubrum* (L.), Coral Reefs, 23, 423–432, 2004.

Mavromatis, V., Schmidt, M., Botz, R., Comas-Bru, L., and Oelkers, E. H.: Experimental quantification of the effect of Mg on calcite–aqueous fluid oxygen isotope fractionation, Chem. Geol., 310–311, 97–105, 2012.

McConnaughey, T.: ^{13}C and ^{18}O isotopic disequilibrium in biological carbonate: II. In vitro simulation of kinetic isotope effects, Geochim. Cosmochim. Ac., 53, 163–171, 1989.

McConnaughey, T. A., Burdett, J., Whelan, J. F., and Charles, K. P.: Carbon isotope in biological carbonates: respiration and photosynthesis, Geochim. Cosmochim. Ac., 61, 611–622, 1997.

McCulloch, M., Fallon, S., Wyndham, T., Hendy, E., Lough, J., and Barnes, D.: Coral record of increased sediment flux to the inner Great Barrier Reef since European settlement, Nature, 421, 727–730, 2003.

McCulloch, M., Trotter, J., Montagna, P., Falter, J., Dunbar, R., Freiwald, A., Försterra, G., Correa, M. L., Maier, C., Rüggeberg, A., and Taviani, M.: Resilience of cold-water scleractinian corals to ocean acidification: boron isotopic systematics of pH and saturation state up-regulation, Geochim. Cosmochim. Ac., 87, 21–34, 2012.

Montaggioni, L. F., Cornec, F. L., Corrège, T., and Cabioch, G.: Coral barium/calcium record of mid-Holocene upwelling activity in New Caledonia, South-West Pacific, Palaeogeogr. Palaeocl., 237, 43–455, 2006.

Montagna, P., McCulloch, M., Taviani, M., Mazzoli, C., and Vendrell, B.: Phosphorus in cold-water corals as a proxy for seawater nutrient chemistry, Science, 312, 1788–1791, 2006.

Morse, J. W., Arvidson, R. S., and Lüttge, A.: Calcium carbonate formation and dissolution, Chem. Rev., 107, 342–381, 2007.

Mucci, A. and Morse, J. W.: The incorporation of Mg^{2+} and Sr^{2+} into calcite overgrowths: influences of growth rate and solution composition, Geochim. Cosmochim. Ac., 47, 217–233, 1983.

Nguyen, T. L., Rahman, M. A., Maki, T., Iwasaki, N., and Hasegawa, H.: Growth characteristics and growth rate estimation of Japanese precious corals, J. Exp. Mar. Biol. Ecol., 441, 117–125, 2013.

Nguyen, T. L., Rahman, M. A., Maki, T., Tamenori, Y., Yoshimura, T., Suzuki, A., Iwasaki, N., and Hasegawa, H.: Distribution of trace elements in Japanese precious coral by XRF and

Ba, B, and U element partitioning in magnesian calcite skeletons

T. Yoshimura et al.

Title Page

Abstract | Introduction

Conclusions | References

Tables | Figures

◀ | ▶

◀ | ▶

Back | Close

Full Screen / Esc

Printer-friendly Version

Interactive Discussion

sulfur speciation by XANES: correlation between trace elements and growth rings, Geochim. Cosmochim. Ac., 127, 1–9, 2014.

Ni, Y., Foster, G. L., Bailey, T., Elliott, T., Schmidt, D. N., Pearson, P. N., Haley, B., and Coath, C.: A core top assessment of proxies for the ocean carbonate system in surface-dwelling foraminifers, Paleoceanography, 22, PA3212, doi:10.1029/2006PA001337, 2007.

Noé, S. U. and Dullo, W.-C.: Skeletal morphogenesis and growth mode of modern and fossil deep-water isidid gorgonians (Octocorallia) in the West Pacific (New Zealand and Sea of Okhotsk), Coral Reefs, 25, 303–320, 2006.

Noé, S. U., Lembke-Jene, L., and Dullo, W.-C.: Varying growth rates in bamboo corals: sclerochronology and radiocarbon dating of a mid Holocene deep-water gorgonian skeleton (*Keratoisis* sp.: Octocorallia) from Chatham Rise (New Zealand), Facies, 54, 151–166, 2008.

Nothdurft, L. D., Webb, G. E., Buster, N. A., Holmes, C. W., and Sorauf, J. E.: Brucite microbialites in living coral skeletons: indicators of extreme microenvironments in shallow-marine settings, Geology, 33, 169–172, 2005.

Oba, T. and Kato, Y.: Section Profile of Barium along 47° N in the North Pacific from the KH-12-4 Cruise, Abstracts of Annual Meeting of the Geochemical Society of Japan 2013, DN/JST.JSTAGE/geochemproc.60.0.203.0, 2012.

Okai, T., Suzuki, A., Terashima, S., Inoue, M., Nohara, M., Kawahata, H., and Imai, N.: Collaborative analysis of GSJ/AIST geochemical reference materials JCp-1 (Coral) and JCt-1 (Giant Clam), Geochemistry, 38, 281–286, 2004 (in Japanese).

Reeder, R. J., Nugent, M., Lamble, G. M., Tait, C. D., and Morris, D. E.: Uranyl incorporation into calcite and aragonite: XAFS and luminescence studies, Environ. Sci. Technol., 34, 638–644, 2000.

Roark, E. B., Guilderson, T. P., Dunbar, R. B., and Ingram, B. L.: Radiocarbon-based ages and growth rates of Hawaiian deep-sea corals, Mar. Ecol.-Prog. Ser., 327, 1–14, 2006.

Rollion-Bard, C., Chaussidon, M., and France-Lanord, C.: pH control on oxygen isotopic composition of symbiotic corals, Earth Planet. Sc. Lett., 215, 275–288, 2003.

Romanek, C., Grossman, E., and Morse, J.: Carbon isotopic fractionation in synthetic calcite, effects of temperature and precipitation rate, Geochim. Cosmochim. Ac., 56, 419–430, 1992.

Russell, A. D., Hönisch, B., Spero, H. J., and Lea, D. W.: Effects of seawater carbonate ion concentration and temperature on shell U, Mg, and Sr in cultured planktonic foraminifera, Geochim. Cosmochim. Ac., 68, 4347–4361, 2004.

Ba, B, and U element partitioning in magnesian calcite skeletons

T. Yoshimura et al.

Title Page

Abstract | Introduction

Conclusions | References

Tables | Figures

◄ | ►

◄ | ►

Back | Close

Full Screen / Esc

Printer-friendly Version

Interactive Discussion

Sanyal, A., Nugent, M., Reeder, R. J., and Bijma, J.: Seawater pH control on the boron isotopic composition of calcite: evidence from inorganic calcite precipitation experiments, Geochim. Cosmochim. Ac., 64, 1551–1555, 2000.

Schauble, E. A., Ghosh, P., and Eiler, J. M.: Preferential formation of ^{13}C–^{18}O bonds in carbonate minerals, estimated using first-principles lattice dynamics, Geochim. Cosmochim. Ac., 70, 2510–2529, 2006.

Sherwood, O. A., Heikoop, J. M., Scott, D. B., Risk, M. J., Guilderson, T. P., and McKinney, R. A.: Stable isotopic composition of deep-sea gorgonian corals *Primnoa* spp.: a new archive of surface processes, Mar. Ecol.-Prog. Ser., 301, 135–148, 2005.

Sinclair, D. J., Allard, G., Williams, B., Ghaleb, B., Ross, S. W., and Risk, M.: Reproducibility of trace element profiles in a specimen of the deep-water bamboo coral *Keratoisis* sp., Geochim. Cosmochim. Ac., 75, 5101–5121, 2011.

Smith, J. E., Risk, M. J., Schwarcz, H. P., and McConnaughey, T. A.: Rapid climate change in the North Atlantic during the Younger Dryas recorded by deep-sea corals, Nature, 386, 818–820, 1997.

Smith, J. E., Schwarcz, H. P., Risk, M. J., McConnaughey, T. A., and Keller, N.: Paleotemperatures from deep-sea corals: overcoming "vital effects", Palaios, 15, 25–32, 2000.

Spero, H. J., Bijma, J., Lea, D. W., and Bemis, B. E.: Effect of seawater carbonate concentration on foraminiferal carbon and oxygen isotopes, Nature, 390, 497–500, 1997.

Tamenori, Y., Yoshimura, T., Nguyen, T. L., Hasegawa, H., Suzuki, A., Kawahata, H., and Iwasaki, N.: Identification of the chemical form of sulfur compounds in the Japanese pink coral (*Corallium elatius*) skeleton using μ-XRF/XAS speciation mapping, J. Struct. Biol., 186, 214–223, 2014.

Tarutani, T., Clayton, R. N., and Mayeda, T. K.: The effect of polymorphism and magnesium substitution on oxygen isotope fractionation between calcium carbonate and water, Geochim. Cosmochim. Ac., 33, 987–996, 1969.

Tesoriero, A. J. and Pankow, J. F.: Solid solution partitioning of Sr^{2+}, Ba^{2+}, and Cd^{2+} to calcite, Geochim. Cosmochim. Ac., 60, 1053–1063, 1996.

Tripati, A. K., Roberts, C. D., Eagle, R. A., and Li, G.: A 20 million year record of planktic foraminiferal B/Ca ratios: systematics and uncertainties in pCO$_2$ reconstructions, Geochim. Cosmochim. Ac., 75, 2582–2610, 2011.

Uchikawa, J. and Zeebe, R. E.: Examining possible effects of seawater pH decline on foraminiferal stable isotopes during the Paleocene–Eocene Thermal Maximum, Paleoceanography, 25, PA2216, doi:10.1029/2009PA001864, 2010.

Usdowski, E. and Hoefs, J.: Oxygen isotope exchange between carbonic acid, bicarbonate, carbonate, and water: a re-examination of the data of McCrea (1950) and an expression for the overall partitioning of oxygen isotopes between the carbonate species and water, Geochim. Cosmochim. Ac., 57, 3815–3818, 1993.

Urey, H.: The thermodynamic properties of isotopic substances, J. Chem. Soc. London, 562–581, 1947.

van de Flierdt, T., Robinson, L. F., Adkins, J. F., Hemming, S. R., and Goldstein, S. L.: Temporal stability of the neodymium isotope signature of the Holocene to glacial North Atlantic, Paleoceanography, 21, PA4102, doi:10.1029/2006PA001294, 2006.

Venn, A. A., Tambutté, E., Holcomb, M., Laurent, J., Allemand, D., and Tambutté, S.: Impact of seawater acidification on pH at the tissue–skeleton interface and calcification in reef corals, P. Natl. Acad. Sci. USA, 110, 1634–1639, 2013.

Vielzeuf, D., Garrabou, J., Gagnon, A., Ricolleau, A., Adkins, J., Günther, D., Hametner, K., Devidal, J.-L., Reusser, E., Perrin, J., and Floquet, N.: Distribution of sulphur and magnesium in the red coral, Chem. Geol., 355, 13–27, 2013.

Wolgemuth, K. and Broecker, W. S.: Barium in sea water, Earth Planet. Sc. Lett., 8, 372–378, 1970.

Yoshimura, T., Tanimizu, M., Inoue, M., Suzuki, A., Iwasaki, N., and Kawahata, H.: Mg isotope fractionation in biogenic carbonates of deep-sea coral, benthic foraminifera, and hermatypic coral, Anal. Bioanal. Chem., 401, 2755–2769, 2011.

Yoshimura, T., Suzuki, A., and Iwasaki, N.: Mechanism of O and C isotope fractionation in magnesian calcite skeletons of Octocorallia corals and an implication on their calcification response to ocean acidification, Biogeosciences Discuss., 12, 389–412, doi:10.5194/bgd-12-389-2015, 2015.

Yu, J., Elderfield, H., and Hönisch, B.: B/Ca in planktonic foraminifera as a proxy for surface seawater pH, Paleoceanography, 22, PA22ccq02, doi:10.1029/2006PA001347, 2007.

Zeebe, R. E.: Kinetic fractionation of carbon and oxygen isotopes during hydration of carbon dioxide, Geochim. Cosmochim. Ac., 139, 540–552, 2014.

Zeebe, R. E., Bijma, J., and Wolf-Gladrow, D. A.: A diffusion–reaction model of carbon isotope fractionation in foraminifera, Mar. Chem. 64, 199–227, 1999a.

Zeebe, R. E., Wolf-Gladrow, D. A., and Jansen, H.: On the time required to establish chemical and isotopic equilibrium in the carbon dioxide system in seawater, Mar. Chem., 65, 135–153, 1999b.

Ba, B, and U element partitioning in magnesian calcite skeletons

T. Yoshimura et al.

Title Page

Abstract | Introduction

Conclusions | References

Tables | Figures

|◀ | ▶|

◀ | ▶

Back | Close

Full Screen / Esc

Printer-friendly Version

Interactive Discussion

Table 1. Sampling locations, water depth and temperature, stable oxygen and carbon isotope ratios, and trace element concentrations of the coral samples. The $\Delta^{18}O$ and $\Delta^{13}C$ were calculated by using isotope fractionation factors for inorganic magnesian calcite (Mavromatis et al., 2012; Jimenez-Lopez, 2006).

Sample ID		Latitude/ Longitude	Depth m	Temp. °C	$\delta^{18}O$ ‰ VPDB	$\Delta^{18}O$ ‰	$\delta^{13}C$ ‰ VPDB	$\Delta^{13}C$ ‰	B/Ca mmol mol^{-1}	Ba/Ca µmol mol^{-1}	U/Ca µmol mol^{-1}	Mg/Ca mmol mol^{-1}
DPC-01	*C. konojoi*	32° N 134° E	100	19.5	−1.80	−2.20	−3.63	−5.38	0.17	5.5	0.09	116.56
DPC-12	*P. japonicum*	32° N 134° E	100	19.5	−1.15	−1.53	0.00	−1.75	0.25	5.0	0.02	116.71
DPC-K1	*P. japonicum*	25° N 126° E	200–300	18.0	−0.73	−1.83	−0.54	−2.00	0.22	4.9	0.02	137.40
DPC-0812	*C. elatius*	25° N 126° E	200–300	18.0	−1.12	−1.94	−0.95	−2.41	0.14	4.4	0.02	121.52
DPC-14	*Keratoisis* sp.	27° N 142° E	700	7.0	0.74	−2.58	−2.10	−2.97	0.17	9.8	0.01	90.93
DPC-K4	*Corallium* sp.	32° N 132° E	100	19.5	−1.61	−2.22	−5.07	−6.81	0.15	5.0	0.04	130.94
DPC-K3	*Corallium* sp.	27° N 142° E	700	6.5	0.24	−3.15	−4.95	−5.82	0.13	9.3	0.01	86.59
DPC-K5	*Corallium* sp.	28° N 177° E	1000	3.5	0.20	−3.89	−6.12	−6.70	0.10	13.9	0.01	78.40
DPC-V1	*Corallium* sp.	9° N 109° E	200–400	10–15	−2.38	−4.66	−5.95	−7.34	0.16	5.7	0.02	113.58
DPC-V4	*Corallium* sp.	9° N 109° E	200–400	10–15	−1.72	−4.06	−4.32	−5.71	0.17	5.2	0.02	117.69
DPC-951	*Corallium* sp.	35° N 139° E	105	17.5	−1.09	−2.10	−4.12	−5.85	0.14	4.7	0.04	123.13

Table 2. Correlation coefficients (r) and p values obtained by regressing δ^{18}O and δ^{13}C, B/Ca, and U/Ca against various parameters. The inorganic carbon data were calculated from alkalinity and total dissolved inorganic carbon data made available by the Global Ocean Data Analysis Project.

		Temp.	pH	pCO$_2$	HCO$_3^-$	CO$_3^{2-}$	HCO$_3^-$/CO$_3^{2-}$	B/Ca	U/Ca
δ^{18}O	r	0.652	0.727	−0.696	−0.750	0.733	−0.620	0.478	0.342
	p	0.0001	0.0059	0.0012	0.0648	0.0000	0.0030	0.0041	0.0001
δ^{13}C	r	0.318	0.332	−0.372	−0.325	0.304	−0.370	0.678	−0.133
	p	0.0042	0.2225	0.0045	0.8117	0.0031	0.0069	0.0007	0.0014
B/Ca	r	0.552	0.542	−0.565	−0.537	0.525	−0.571	–	0.095
	p	0.0049	0.1818	0.0000	0.0080	0.0020	0.0000	–	0.0000
U/Ca	r	0.576	0.614	−0.545	−0.635	0.645	−0.537	0.095	–
	p	0.6994	0.0565	0.0031	0.0175	0.6463	0.0039	0.6092	–

Ba, B, and U element partitioning in magnesian calcite skeletons

T. Yoshimura et al.

Table 3. Trace element (B, Ba, and U) concentrations in a semi-fossilized coral (specimen DPC-15 *Corallium elatius*, Fig. 1). Sample #1 was obtained at the central axis and sample #17 was at the outermost.

Sample ID	B/Ca $\mathrm{mmol\,mol^{-1}}$	Ba/Ca $\mathrm{\mu mol\,mol^{-1}}$	U/Ca $\mathrm{\mu mol\,mol^{-1}}$	Mg/Ca $\mathrm{mmol\,mol^{-1}}$
DPC-K15-1	0.16	5.3	0.03	128.39
DPC-K15-2	0.17	4.8	0.04	127.92
DPC-K15-3	0.14	4.6	0.03	124.44
DPC-K15-4	0.12	4.4	0.09	126.92
DPC-K15-5	0.12	4.5	0.13	127.85
DPC-K15-6	0.12	4.5	0.10	125.40
DPC-K15-7	0.11	4.6	0.08	125.87
DPC-K15-8	0.11	4.4	0.12	127.01
DPC-K15-9	0.11	4.4	0.12	124.21
DPC-K15-10	0.11	4.5	0.21	125.56
DPC-K15-11	0.11	4.6	0.21	128.26
DPC-K15-12	0.10	4.4	0.33	122.40
DPC-K15-13	0.11	4.5	0.31	124.30
DPC-K15-14	0.11	4.6	0.23	126.35
DPC-K15-15	0.13	4.8	0.19	129.81
DPC-K15-16	0.11	4.5	0.27	127.25
DPC-K15-17	0.11	4.6	0.22	126.76

Figure 1. Photograph of a specimen of the deep-sea coral DPC-11 *Corallium elatius* (left), and a cross section of a semi-fossilized specimen DPC-15 *C. elatius* (right). The white arrow denotes the transect along which samples were obtained by micromilling (17 mm in length). The outermost part of the DPC-15 skeleton was not sampled because of notable bioerosion caused by marine sponges.
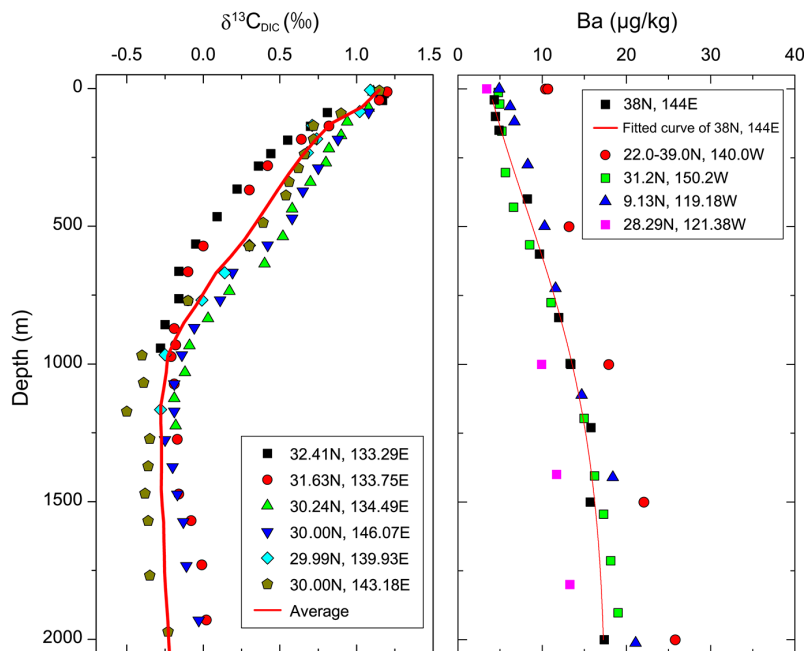
Figure 2. Comparison of $\delta^{13}C_{DIC}$–depth and [Ba^{2+}]–depth relationships among North Pacific sites. We selected published data collected at points close to the sampling localities of the corals analyzed in this study. The $\delta^{13}C$ carbon data were collected along sections P02, P09, and P10 in the Pacific Ocean distributed by the Global Ocean Data Analysis Project. The $\delta^{13}C_{DIC}$ values used to evaluate proxies were estimated from the curve obtained by averaging data from the Northwest Pacific sites. Values from a curve fitted to dissolved Ba concentrations from the western Pacific (38° N–144° E, Oba and Kato, 2012) were used for the Ba/Ca proxy calibration. Published [Ba^{2+}] data from GEOSECS cruises of eastern Pacific sampling stations (green squares, Chan et al., 1976; blue triangles, Bernat et al., 1972; purple squares, Bender et al., 1972; and red circles, Wolgemuth and Broecker, 1970) are also plotted for reference.

Title Page

Abstract | Introduction

Conclusions | References

Tables | Figures

|◄ | ►|

◄ | ►

Back | Close

Full Screen / Esc

Printer-friendly Version

Interactive Discussion

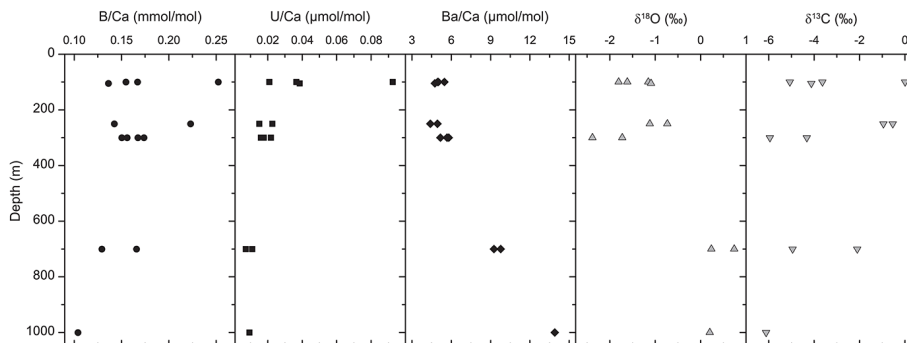**Figure 3.** Scatter plots of B/Ca, Ba/Ca, U/Ca, δ^{18}O and δ^{13}C of Octocorallia corals vs. their habitat depth. The oxygen and carbon isotope data of the specimens are previously published in Yoshimura et al. (2015).
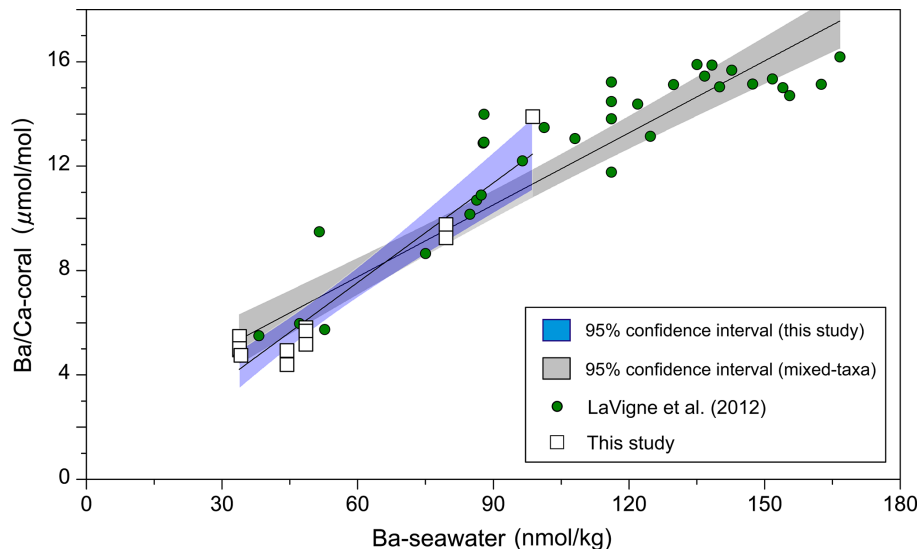
Figure 4. Measured Ba/Ca ratios of high-Mg calcite skeletons of Octocorallia corals (Ba/Ca$_{coral}$) plotted against dissolved Ba concentrations ([Ba]$_{sw}$) from Oba and Kato (2012). For comparison, data from Lavigne et al. (2012) are also shown. The solid lines are regression Eq. (1) (see text), Ba/Ca$_{coral}$ = (0.127 ± 0.012) · [Ba]$_{sw}$ − (0.093 ± 0.688) (r = 0.95; n = 13; p < 0.0001), and regression Eq. (2) for multiple taxa calibration, Ba/Ca$_{coral}$ = (0.092 ± 0.013) · [Ba]$_{sw}$ + (2.246 ± 1.334) (r = 0.906, n = 46, p < 0.0001). It is noteworthy that the multi-taxa calibration equation for aragonitic cold-water scleractinian corals published by Anagnostou et al. (2011), Ba/Ca$_{coral}$ = (0.104 ± 0.024) · [Ba]$_{sw}$ + (2.415 ± 1.536), agrees well with these equations for calcitic corals.
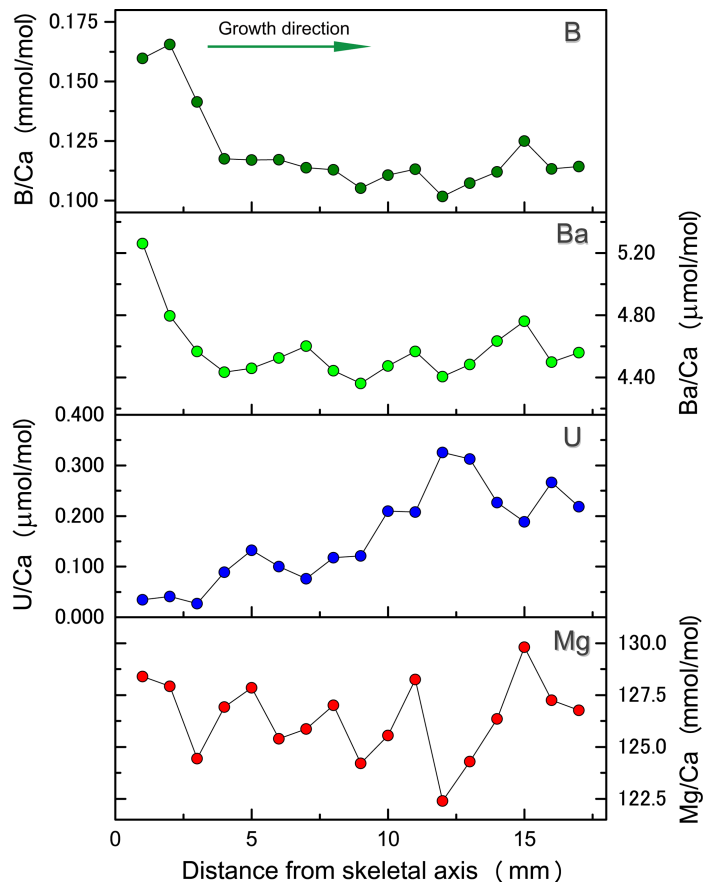
Figure 5. Profiles of B/Ca, Ba/Ca, U/Ca, and Mg/Ca along the growth transect of a semi-fossilized specimen of *Corallium elatius*. A slab cut perpendicular to the growth axis was sampled with a micromill drill along the growth transect at 1 mm intervals from the central axis to the margin (white arrow in Fig. 1).

Title Page

Abstract | Introduction

Conclusions | References

Tables | Figures

|◄ | ►|

◄ | ►

Back | Close

Full Screen / Esc

Printer-friendly Version
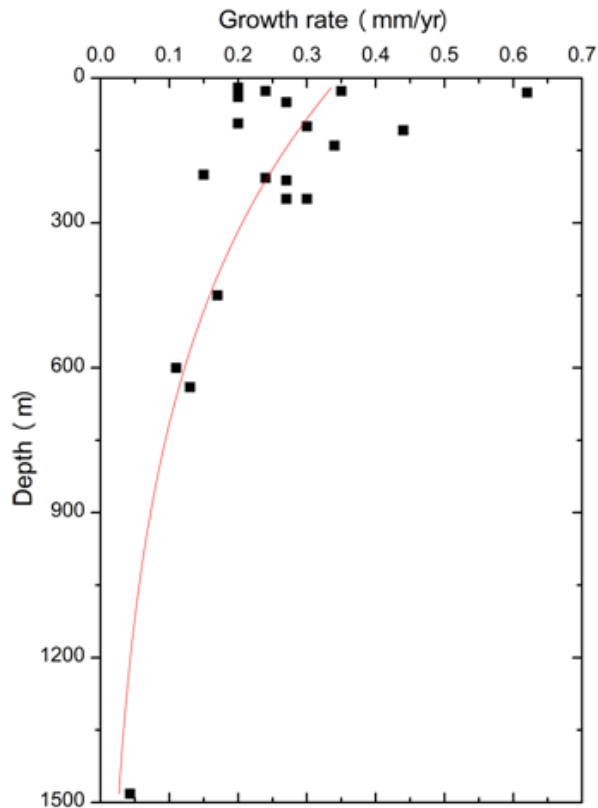
Interactive Discussion

Figure 6. Relationship between water depth and growth rate in Octocorallia Corallidae corals. The solid line is the linear regression obtained using published data for various taxa (Griffin and Druffel, 1989; Druffel et al., 1990; Garrabou and Harmelin, 2002; Marschal et al., 2004; Andrews et al., 2005; Bramanti et al., 2005; Roark et al., 2006; Bruckner and Roberts, 2009; Gallmetzer et al., 2010; Nguyen et al., 2013; Vielzeuf et al., 2013). The curve is an exponential fit through data of a growth rate change (y) and meter of depth (x): $y = -0.022 + 0.360 \cdot \exp(-0.0012 \cdot x)$.